Electronic Supplementary Material (ESI) for Organic & Biomolecular Chemistry

Preferences of rhodamine coupled (aminoalkyl)-piperazine probes towards Hg(II) ion and their FRET mediated signaling

Biswonath Biswal and Bamaprasad Bag*

Colloids and Materials Chemistry Department, CSIR-Institute of Minerals and Materials Technology, P.O.: R.R.L., Bhubaneswar-751 013, Odisha, India. Email: *bpbag@immt.res.in*

Supplementary information

Materials and Methods

All the reagent grade chemicals were used without purification unless otherwise specified. Rhodamine B, rhodamine-6G, 1,4-*bis*-(aminopropyl)-piperazine, anthracene-9-carboxaldehyde, 4-chloro-7-nitrobenzofurazan, 1-(2-aminoethyl)-piperazine and metal perchlorate salts were obtained from Sigma-Aldrich (USA) and used as received. Anhydrous sodium sulfate, sodium borohydride, triethylamine, acids, buffers and the solvents were received from S. D. Fine Chemicals (India). All the solvents were freshly distilled prior to use following the literature procedures and the reactions were carried out under N_2 atmosphere. Chromatographic separations were done by column chromatography using 100–200 mesh silica gel.

The compounds were characterized by elemental analyses, ^{1}H-NMR, ^{13}C-NMR and mass (ESI) spectroscopy. ^{1}H-NMR and ^{13}C-NMR spectra were recorded on a JEOL JNM-AL400 FT V4.0 AL 400 (400 MHz and 100 MHz respectively) instrument in $CDCl_3$ with Me_4Si as the internal standard. Electrospray mass spectral data were recorded on a MICROMASS QUATTRO II triple quadruple mass spectrometer. The dissolved samples of the compounds in suitable solvents were introduced into the ESI source through a syringe pump at the rate of 5μL/min, ESI capillary was set at 3.5 kV with 40V cone voltage and the spectra were recorded at 6 s scans. Melting points were determined with a melting point apparatus by PERFIT, India and were uncorrected. Elemental analyses were done in an Elementar Vario EL III Carlo Erba 1108 elemental analyzer. UV-visible spectra were recorded on a Perkin Elmer Lambda 650 UV/VIS spectrophotometer at 298 K in 10^{-4}-10^{-6} M concentration. Steady-state fluorescence spectra were obtained with a Fluoromax 4P spectrofluorometer at 298 K. The solid-state emission spectra were also recorded in Fluoromax 4P spectrofluorometer at 298K excited at requisite wavelength with 450WXenon lamp, band pass 2 nm and slapped through 1 nm during recording the spectra with integration time 0.2 s.

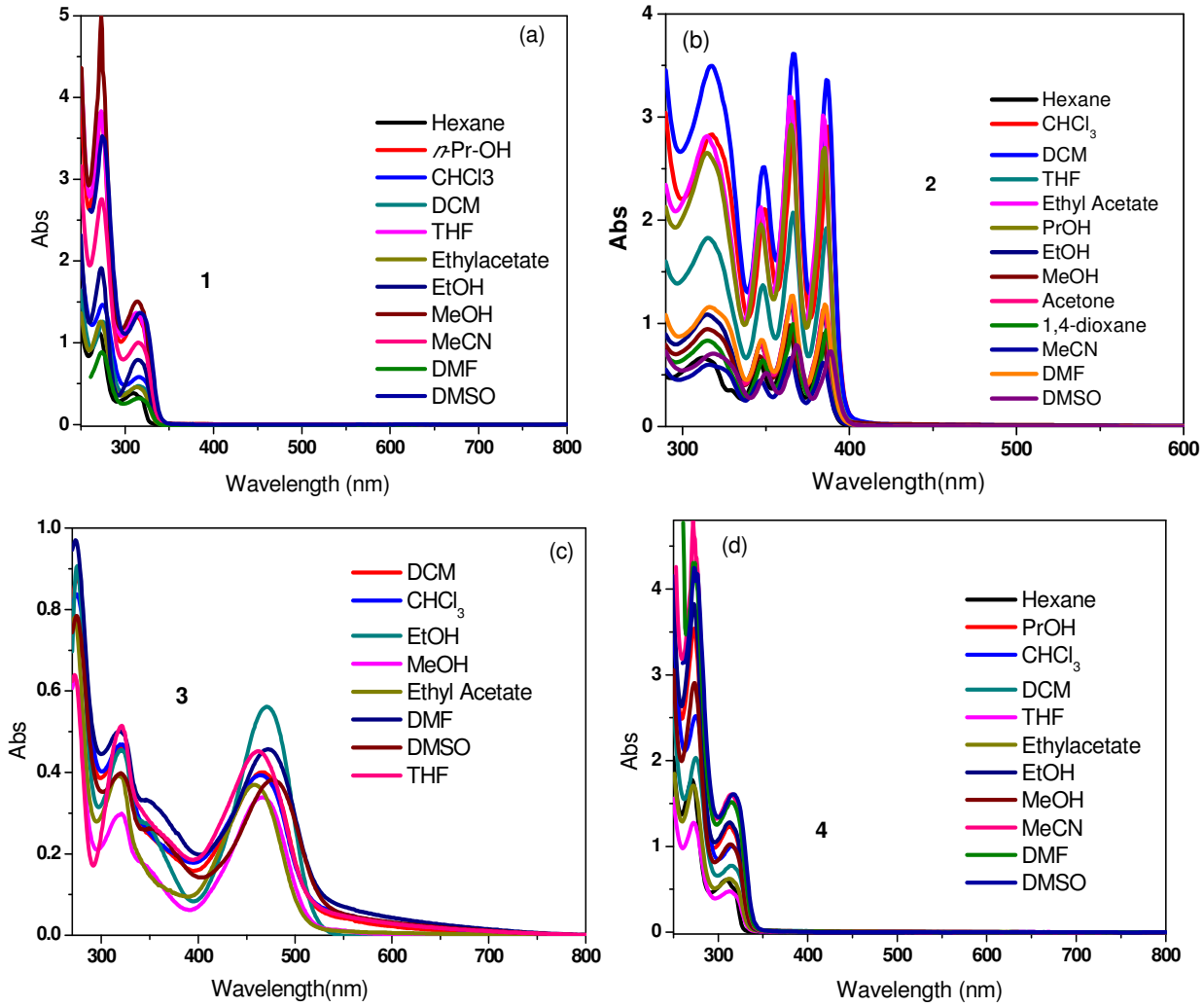

Fig. S1: Absorption spectra of **1** - **4** in various solvents. Conc. of probes: 1×10^{-4} M (for **1**, **2** and **4**) and 1×10^{-5} M (for **3**).

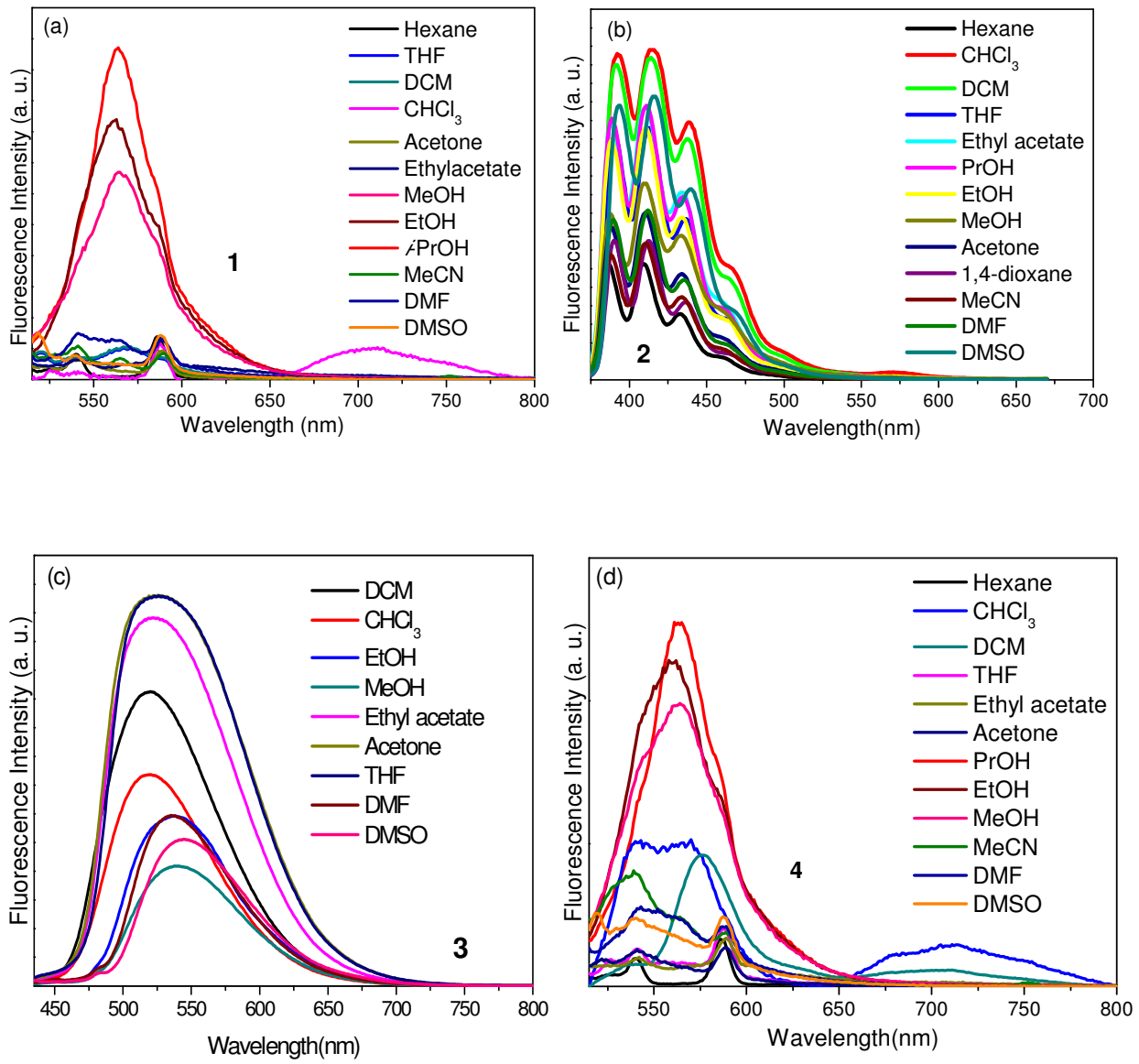

Fig. S2: Fluorescence spectra of (a) **1**, (b) **2**, (c) **3** and (d) **4** in different solvents. Concentration of the probes: [**1**] = 1×10^{-7} M, [**2**] = 1×10^{-6} M, [**3**] = 1×10^{-6} M and [**4**] = 1×10^{-7} M; λ_{ex} = 500 nm for **1** and **4**, 365nm for **2** and 420nm for **3** respectively; emission and excitation band pass = 5nm; T= 298 K; The error in fluorescence spectral data is within 10 %. The fluorescence quantum yields (ϕ_F) were calculated by comparison of corrected spectrum with that of rhodamine G (ϕ_F = 0.95) in EtOH taking the area under the total emission, which was calculated to be < 0.001 in each case.

Table ST1: Absorption peak position (λ, nm), corresponding molar extinction coefficients (ε, $dm^3\ mol^{-1}\ cm^{-1}$) and emission maxima of the probes **1-4** in different solvents.

Probe	Solvent	λ_{abs}, nm (ε, $dm^3\ mol^{-1}\ cm^{-1}$)	λ_{em} [a]	Probe	λ_{abs}, nm (ε, $dm^3\ mol^{-1}\ cm^{-1}$)	λ_{em} [a]
1	Hexane	271 (11231), 310 (3905)	539, 587	**4**	270 (n. d.), 310 (n. d.)	539,587
	DCM	276 (12483), 317 (4685)	575		276 (20085), 315 (7779)	576
	$CHCl_3$	276 (14509), 317 (5719)	569		273 (25207), 317 (9890)	541,579
	THF	273 (38227), 312 (13539)	588		273 (12655), 314 (4682)	587
	Acetone	413 (741)	540,587		n. d.	540, 588
	1,4-dioxane	273 (21548), 312 (7650)	540,586		273 (33272), 312 (11824)	539,589
	Ethylacetate	273 (12507), 312 (4523)	587		271 (17155), 312 (6272)	588
	MeCN	274 (27067), 315 (9898)	539,589		273 (48044), 317 (15685)	540
	MeOH	273 (49370), 314 (15056)	564		273 (28721), 315 (10140)	564
	EtOH	273 (19056), 315 (7780)	561		272 (37808), 314 (12584)	559
	i-PrOH	273 (37887), 314 (13199)	560		273 (35028), 312 (12134)	563
	DMF	273 (8769), 317 (3182)	540,588		274 (42887), 315 (15162)	542,587
	DMSO	274 (35078), 320 (13404)	539,587		274 (41780), 317 (16101)	540,588

Probe	Solvent	λ_{abs}, nm (ε, $dm^3\ mol^{-1}\ cm^{-1}$)	λ_{em} [b]
2	Hexane	270 (n. d.), 312 (n. d.), 345 (n. d.), 364 (n. d.), 383 (n. d.)	387, 409, 433
	DCM	317 (35033), 348 (25359), 366 (36056), 386 (35230)	391, 141, 440
	$CHCl_3$	317 (28033), 368(30904), 388 (28662), 349 (20837)	392, 141, 440
	THF	279 (33719), 314 (18053), 348 (13671), 366 (20536), 386 (18820)	390, 412, 437
	Acetone	347 (8191), 365 (11988), 385 (10820)	388, 411, 434
	1,4-dioxane	315 (8179), 348 (6258), 366 (9595), 385 (9224)	388, 412, 437
	Ethylacetate	314 (28033), 347 (21073), 364 (31533), 385 (30275)	387, 409, 436
	MeCN	272 (15011), 323 (5845), 364 (6429), 383 (6028)	387, 411, 434
	MeOH	272 (23146), 317 (9353), 345 (6573), 364 (9454), 383(8623)	387, 409, 432
	EtOH	271 (27974), 315 (10629), 347 (7744), 364 (11578), 385 (10811)	388, 410, 432
	i-PrOH	315 (26382), 347 (19421), 365 (28859), 385 (26814)	388, 410, 433
	DMF	320 (11617), 348 (8117), 365 (12404), 385 (11382)	389, 412, 436
	DMSO	321 (7025), 350 (4724), 368 (7573), 388 (7025)	393, 415, 440
3	Hexane	274 (n.d.), 322 (n. d.), 463 (n. d.)	518 [c]
	DCM	274 (87292), 321 (46235), 467 (40022)	520 [c]
	$CHCl_3$	274 (83202), 320 (47887), 467 (39235)	528 [c]
	THF	271 (63460), 321 (51112), 463 (44977)	525 [c]
	Acetone	345 (7230), 478 (17658)	521 [c]
	1,4-dioxane	273 (3769), 320 (1555), 470 (1768)	540 [c]
	Ethylacetate	273 (78061), 318 (39685), 460 (36780)	543 [c]
	MeCN	273 (18702), 320 (9280), 467 (9365)	540 [c]
	MeOH	276 (89775), 321 (46629), 470 (56404)	539 [c]
	EtOH	273(62536), 320(29634), 467(33837)	537 [c]
	i-PrOH	273 (26718), 316 (11373), 346 (s, 4079), 475 (11077)	535 [c]
	DMF	276 (96533), 321 (49162), 474 (45629)	533 [c]
	DMSO	273 (78005), 323 (39747), 477 (38398)	533 [c]

λ_{ex} = [a] 500nm, [b] 365nm and [c] 420nm.

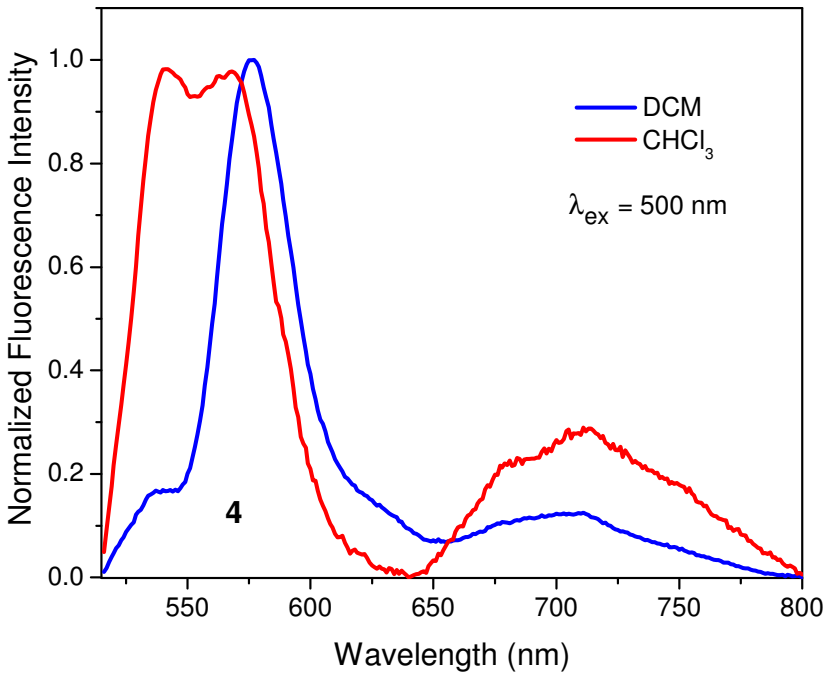

Fig. S3: Normalized fluorescence spectra of **4** alone in $CHCl_3$ and DCM (~ 1×10^{-7} M) upon excitation at 500nm, showing broad structure-less exciplex like emission at 710nm.

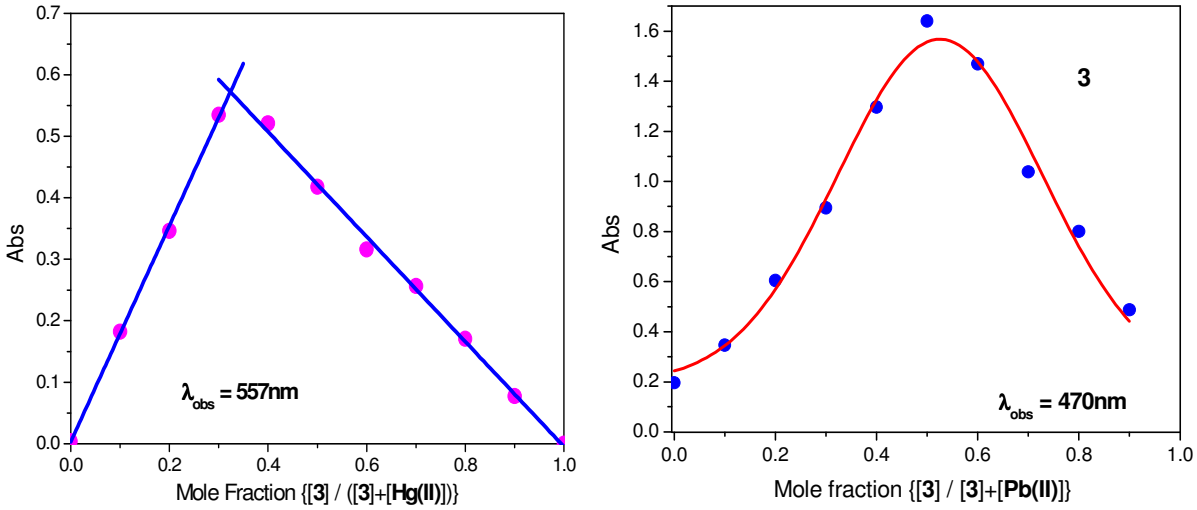

Fig. S4: Complexation stoichiometry determination as a function of change in absorption of **3** as a function of mole fraction of added metal ion in MeCN-H_2O (9:1 v/v). It exhibited 1:2 Ligand-Metal stoichiometry of complexation when observed at 557nm (a) with Hg(II) ion, however, an 1:1 (L:M) stoichiometry was observed on monitoring at 470nm (b) with Pb(II) ion. This renders insight to the step-wise complexation of both Hg(II) ion to **3** in its 'amino-propyl-amino' receptors.

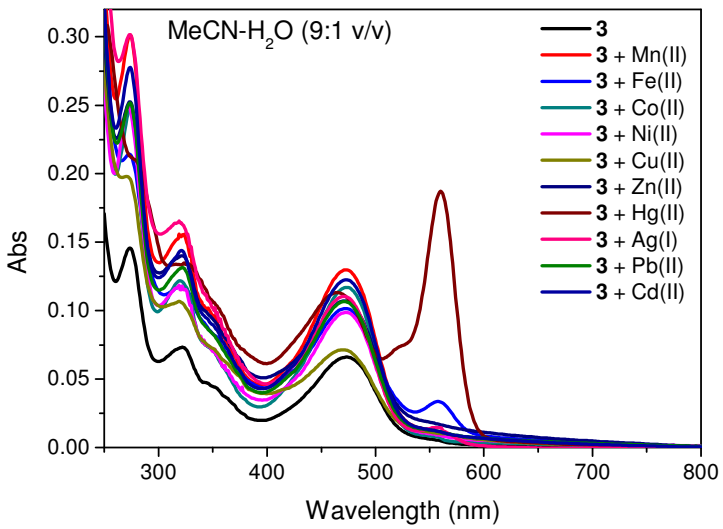

Fig. S5: Absorption spectra of **3** alone and in presence of various metal ions in MeCN-H_2O (9:1 v/v). [**3**]: 1×10^{-5} M, [M(I/II)]: 1×10^{-4} M.

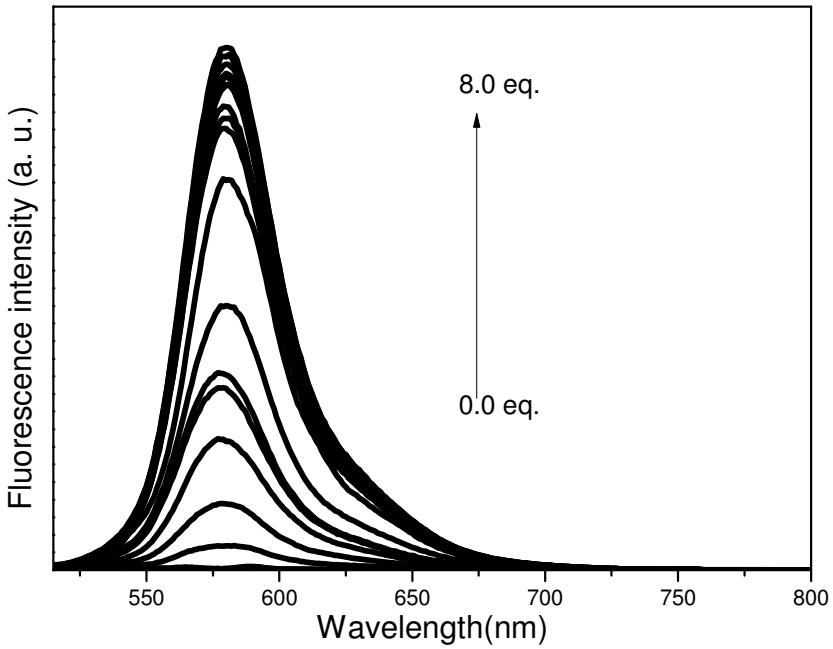

Fig. S6: Fluorescence spectra of **1** alone and in presence of various equivalents of added Hg(II) metal ions in MeCN-H_2O (9:1 v/v), [**1**]: 1×10^{-6} M, λ_{ex} = 500nm, RT, *ex* and *em* b. p. = 5nm.

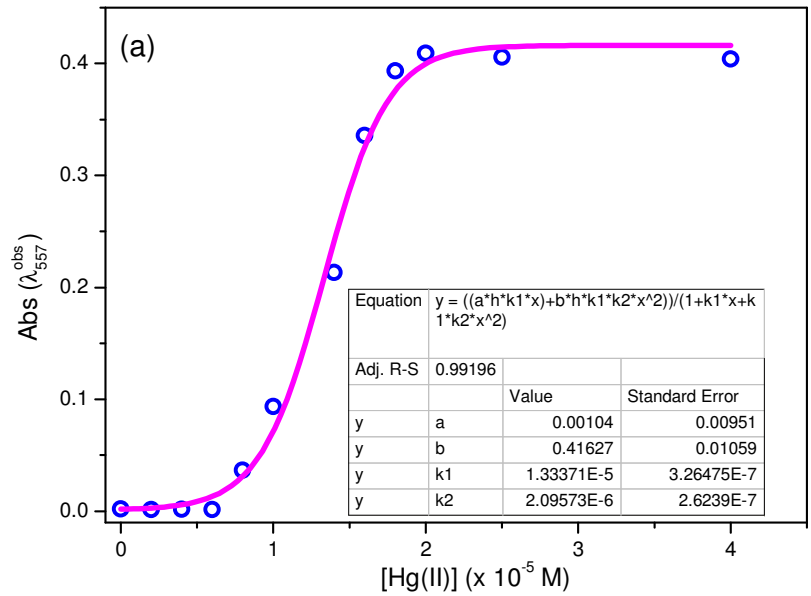

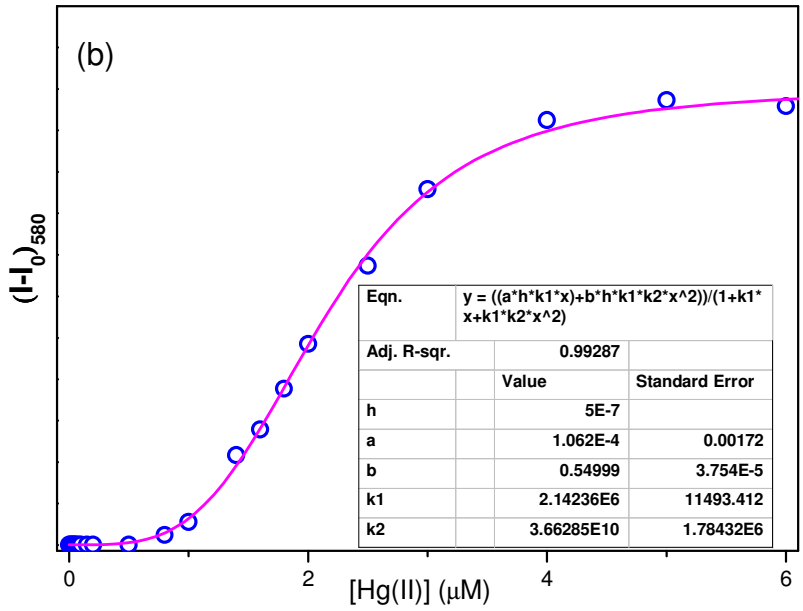

Fig. S7: Plot of change in (a) absorbance and (b) fluorescence intensity of **1** as a function of added [Hg(II)] ions in MeCN-H_2O (9:1 v/v). Experimental conditions: Emission; [**1**]= 5×10^{-7} M, λ_{ex} = 500nm, RT, *ex.* and *em.* b. p. = 5nm; Absorption: [**1**]= 2×10^{-5} M. The plots determine the binding constants k_1 and k_2 for step-wise complexation of both Hg(II) ion and exhibit their positive cooperativity of complexation with **1**.

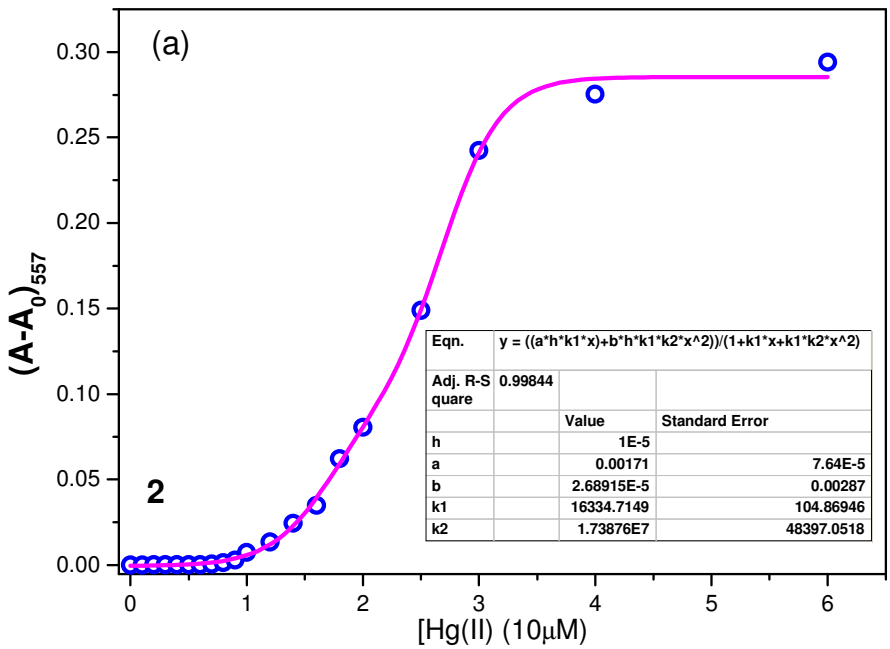

Fig. S8: Plot of change in absorbance of **2** as a function of added [Hg(II)] ion concentration in MeCN-H_2O (9:1 v/v), [**2**] = 1×10^{-5} M.

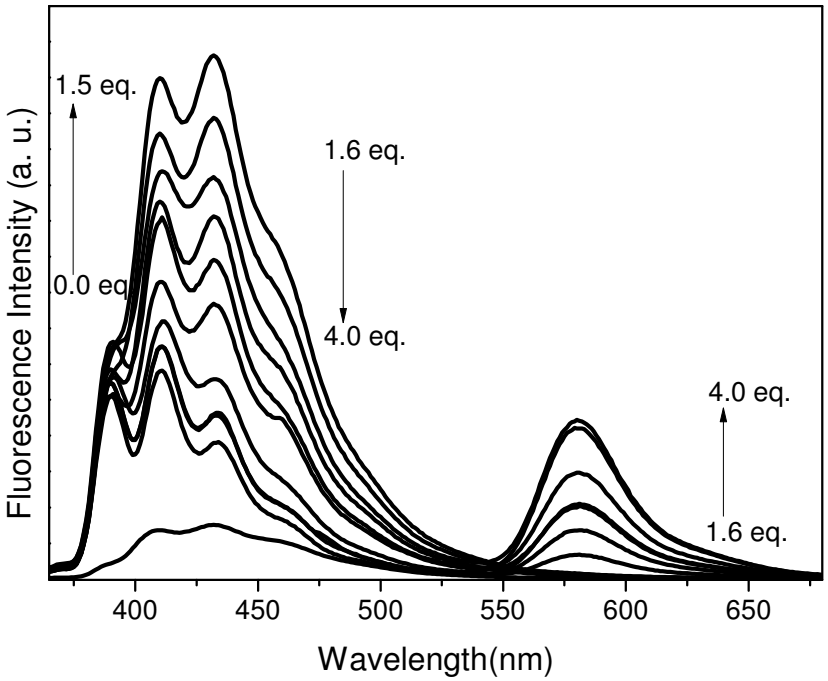

Fig. S9: Fluorescence spectra of **2** alone and in presence of various equivalents of added Hg(II) metal ions in MeCN-H_2O (9:1 v/v), [**2**]: 1×10^{-6} M, λ_{ex} = 365nm, RT, *ex* and *em* b. p. = 5nm.

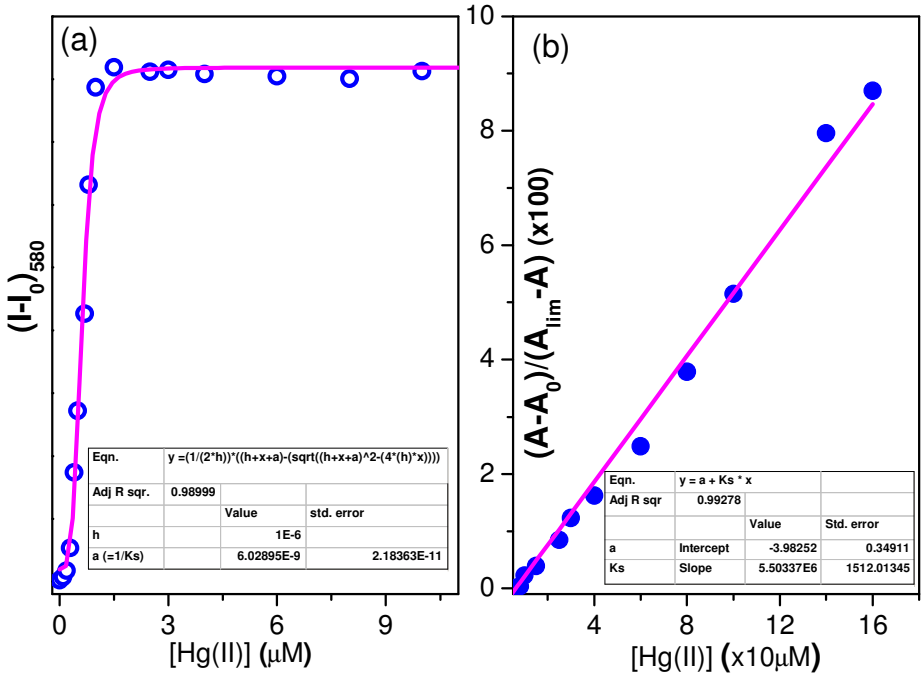

Fig. S10: Plot of change in (a) absorbance and (b) fluorescence intensity of **4** as a function of added [Hg(II)] ion concentration in MeCN-H_2O (9:1 v/v). Experimental conditions: Emission; [**4**]= 1×10^{-6} M, λ_{ex} = 500nm, RT, *ex* and *em* b. p. = 5nm; Absorption: [**4**]= 1×10^{-5} M.

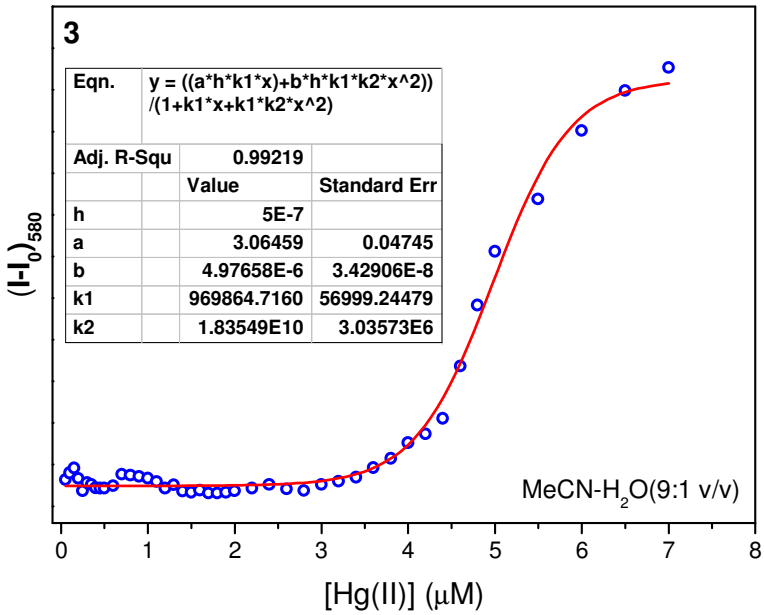

Fig. S11: Plot of change in fluorescence intensity (I_{580}) of **3** as a function of added [Hg(II)] ion concentration in MeCN-H_2O (9:1 v/v). Experimental conditions: Emission; [**3**]= 5×10^{-7} M, λ_{ex} = 465nm, RT, *ex* and *em* b. p. = 5nm.

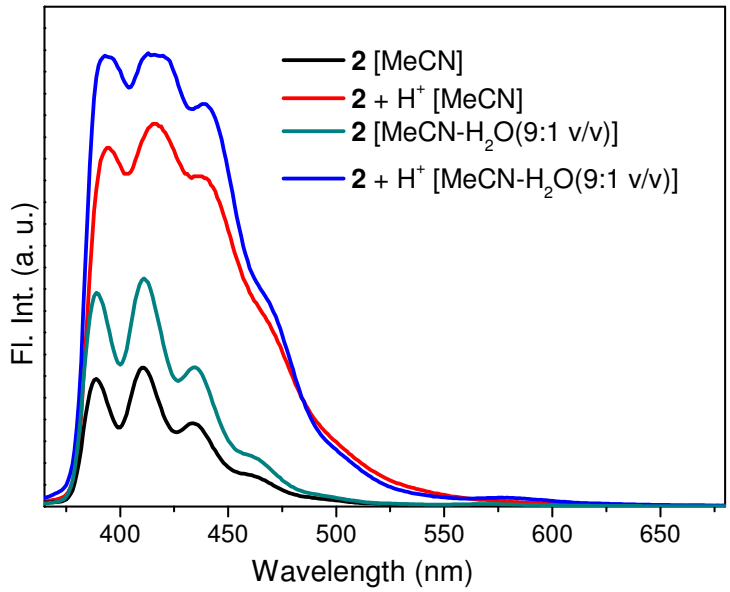

Fig. S12: Fluorescence spectra of **2** alone and in presence protons (H^+) in both MeCN and MeCN-H_2O (9:1 v/v), [**2**]: 1×10^{-6} M, λ_{ex} = 365nm, RT, *ex* and *em* b. p. = 5nm.

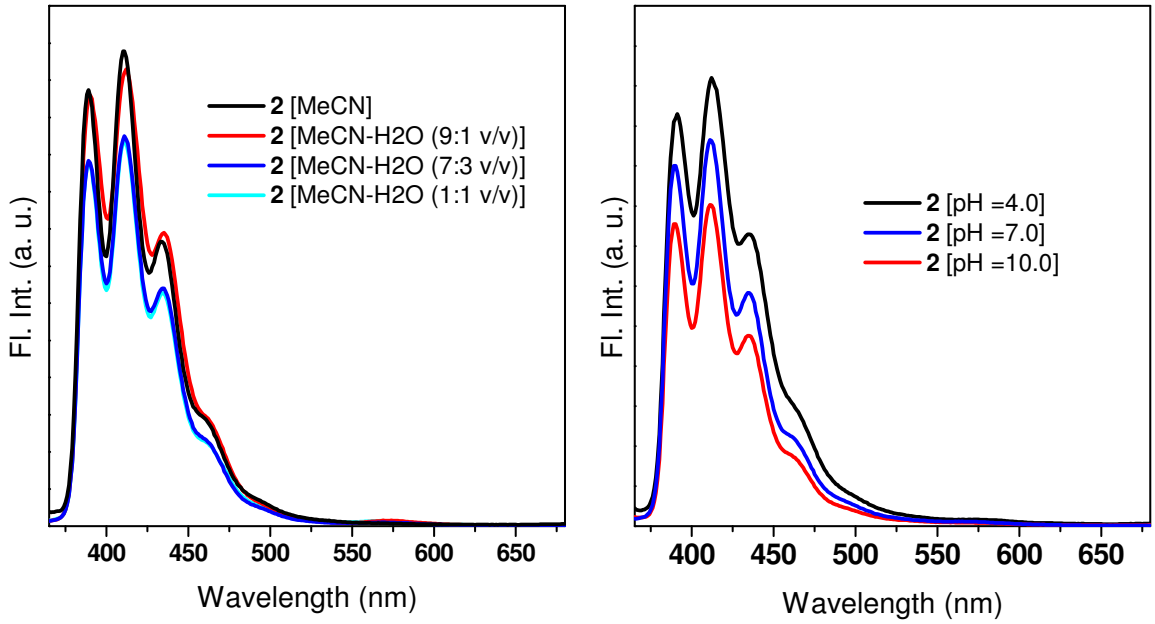

Fig. S13: Fluorescence spectra of **2** in (a) various propertions of aqueous – organic mixture (MeCN-H_2O) and (b) at different pH. [**2**]: 1×10^{-6} M, λ_{ex} = 365nm, RT, *ex* and *em* b. p. = 5nm.

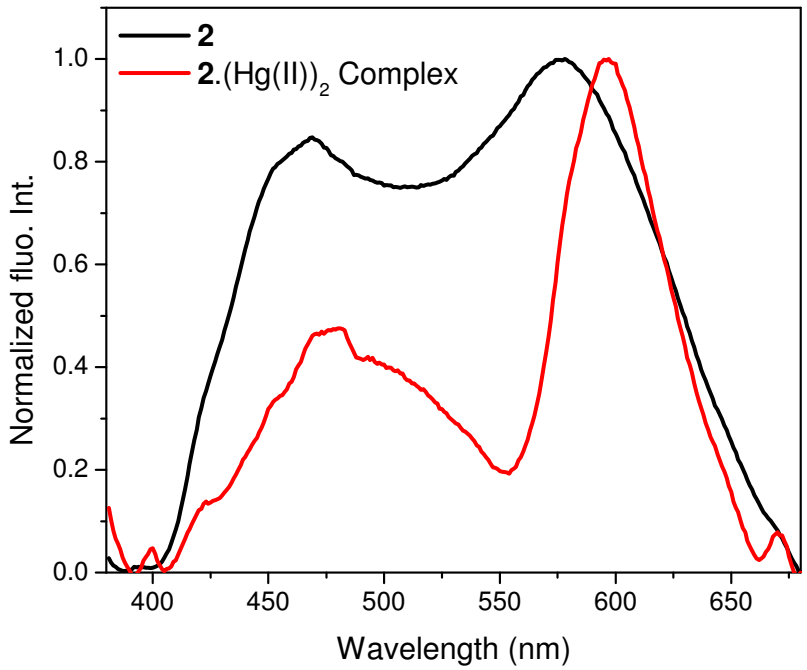

Fig. S14: Normalized solid state fluorescence spectra of **2** and its Hg(II)-complex (λ_{ex} = 365nm).

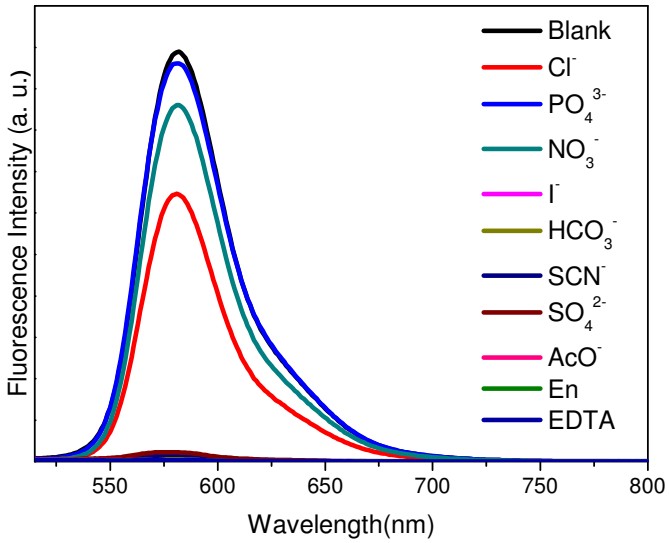

Fig. 15: Fluorescence spectral of saturated solution containing **1** (1 equiv.) and Hg^{II} (5 equiv.) upon addition of various anions (10 equiv.) and chelating agents such as ethylenediamine and EDTA. [**1**] = 5×10^{-7} M, MeCN-H_2O (9:1 v/v), [**2**]: 1×10^{-6} M, λ_{ex} = 500nm, RT, *ex* / *em* b. p. = 5 nm.

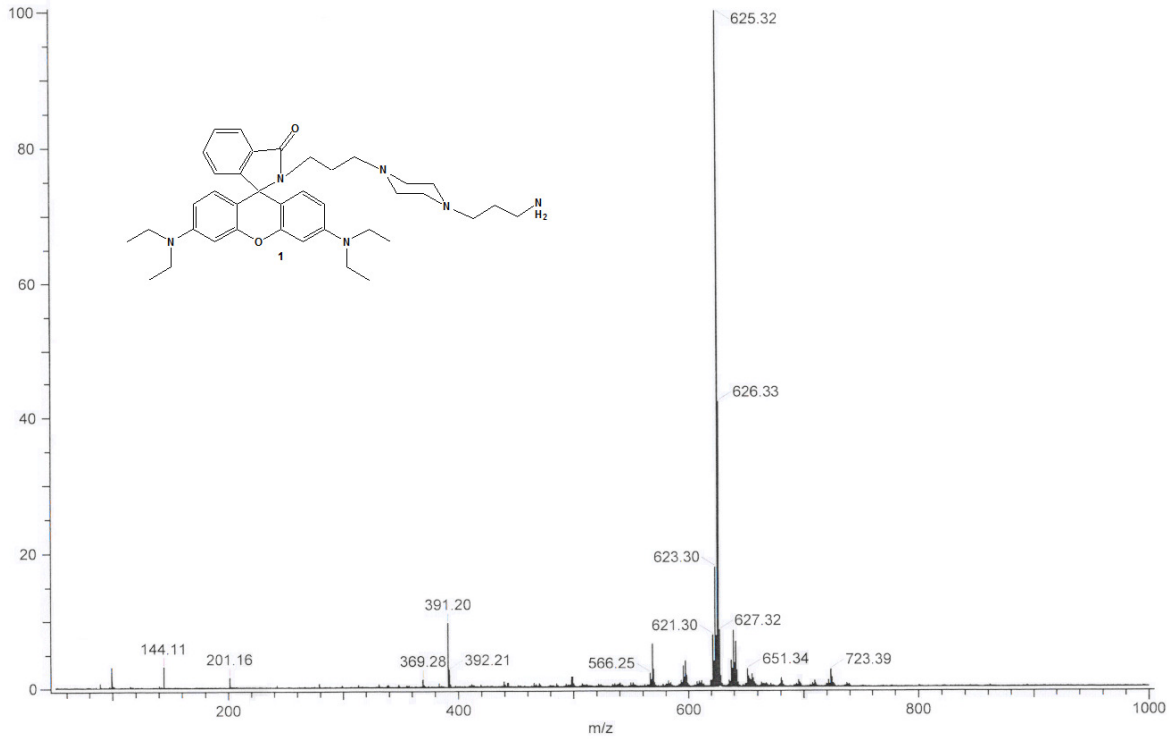

Fig. S16: ESI-MS of **1**.

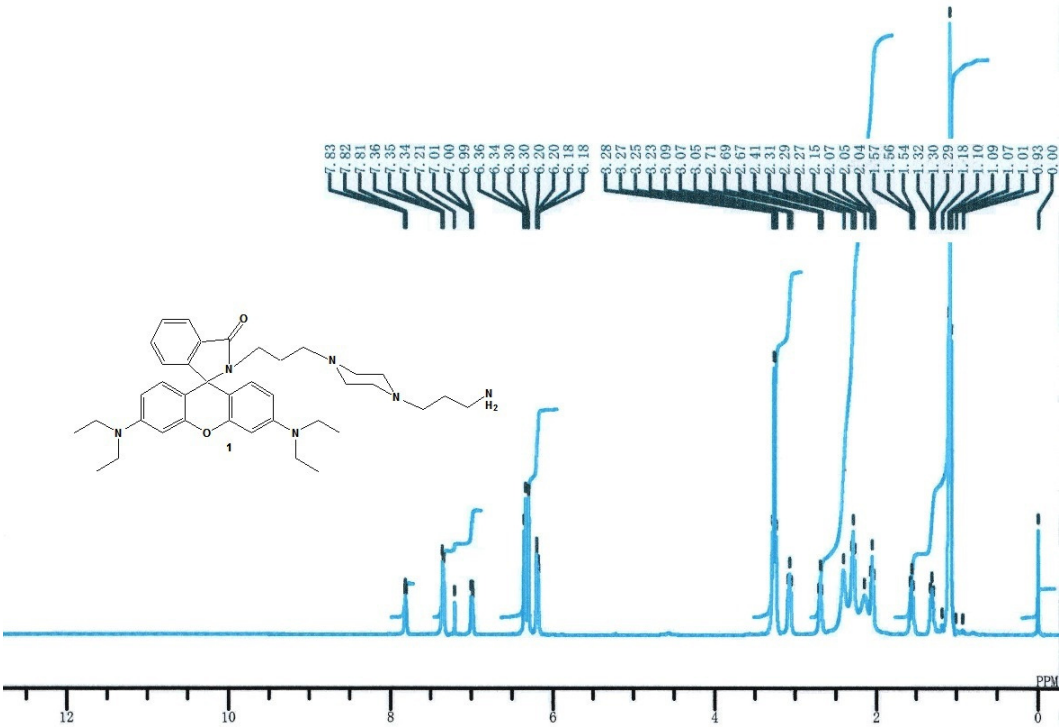

Fig. S17: ^{1}H-NMR spectra of **1** in $CDCl_3$

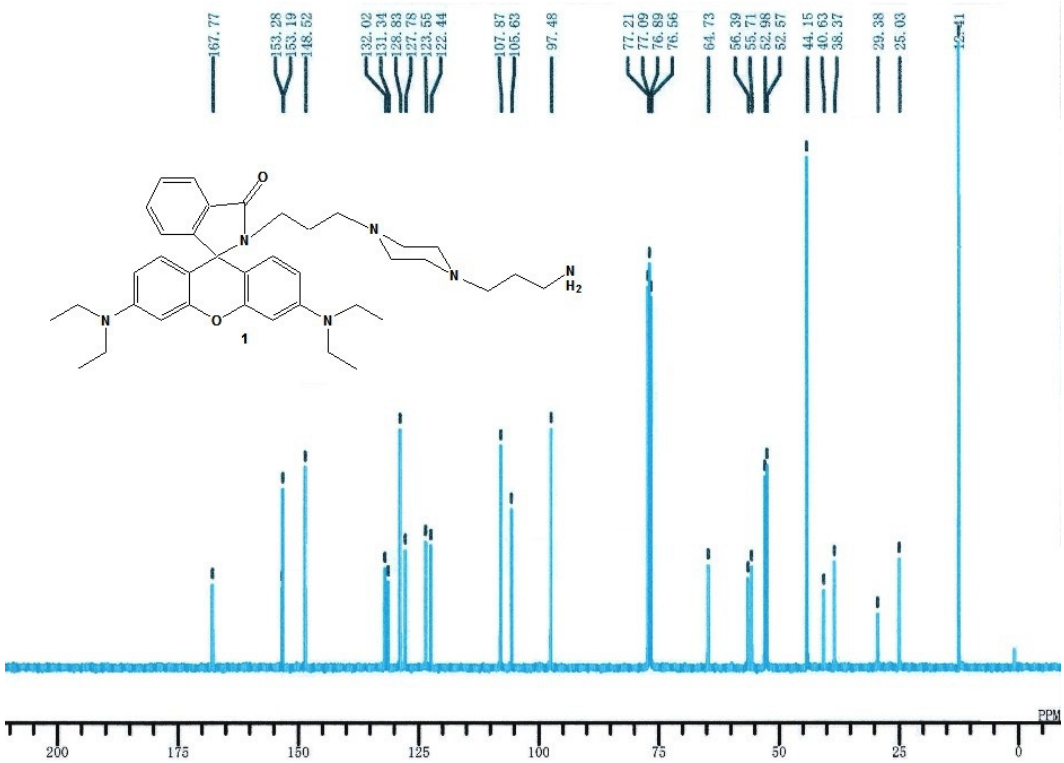

Fig. S18 :^{13}C-NMR spectra of **1** in $CDCl_3$.

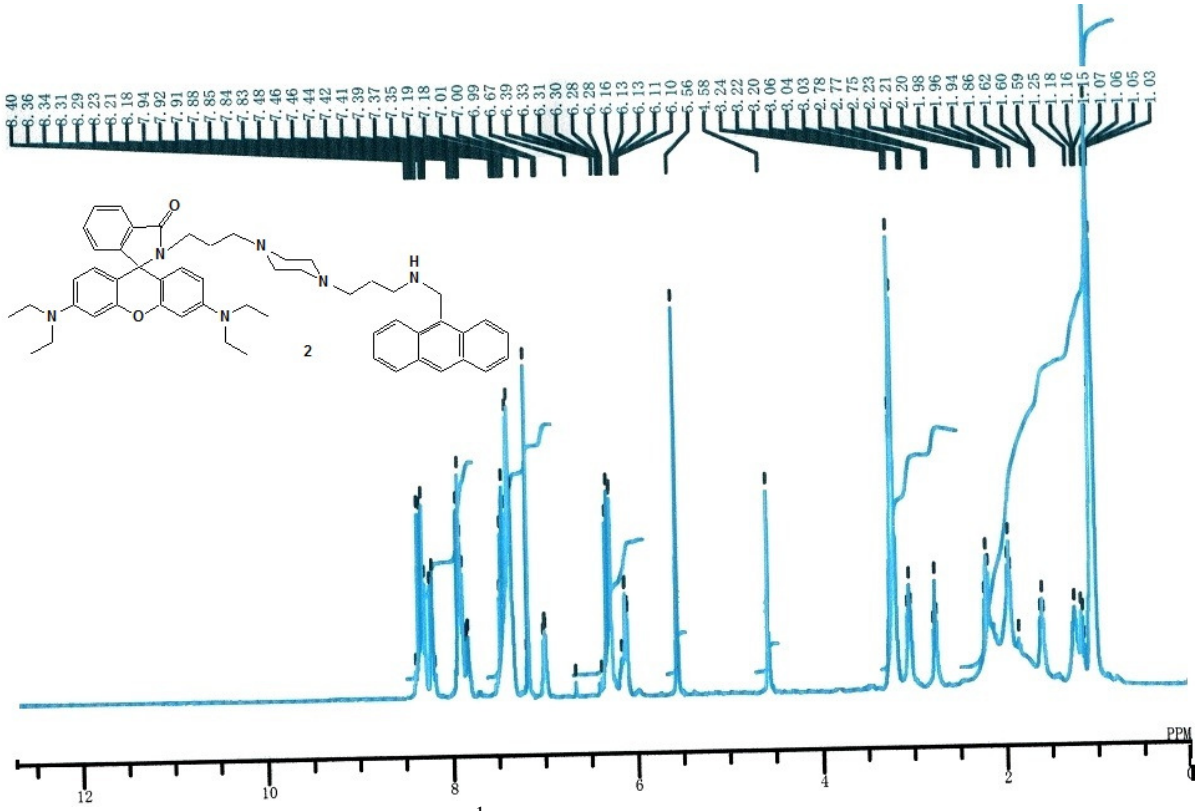

Fig. S19: ^{1}H-NMR spectra of **2** in $CDCl_3$.

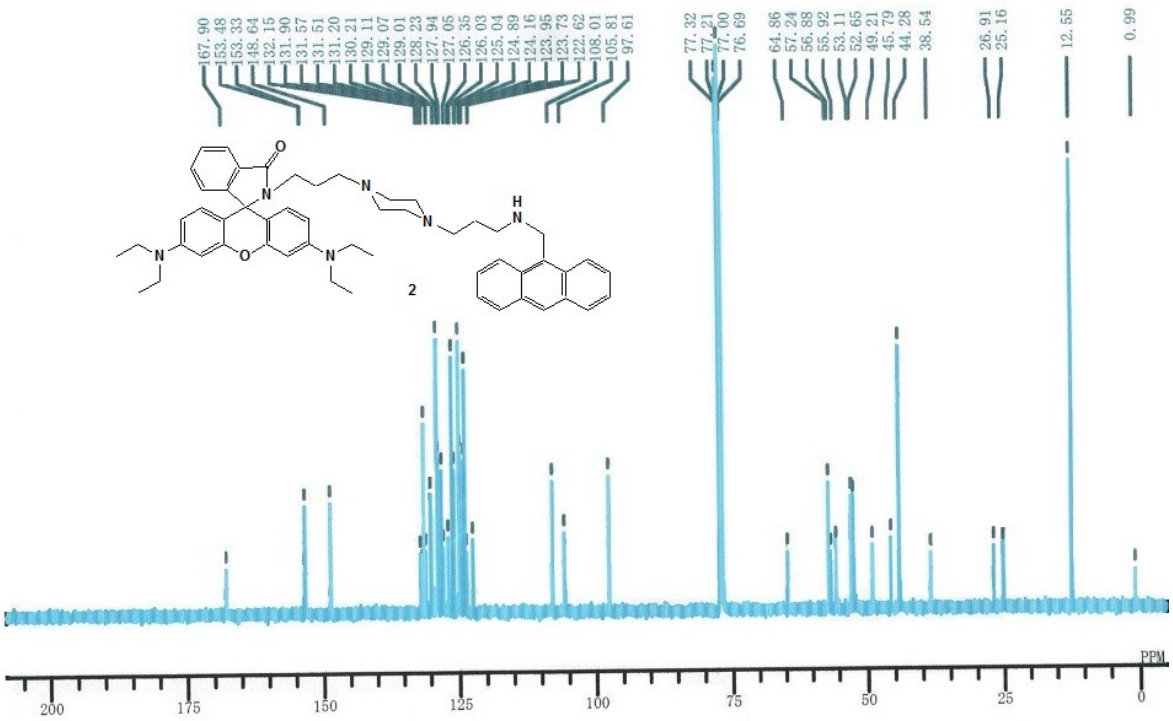

Fig. S20: ^{13}C-NMR spectra of **2** in $CDCl_3$

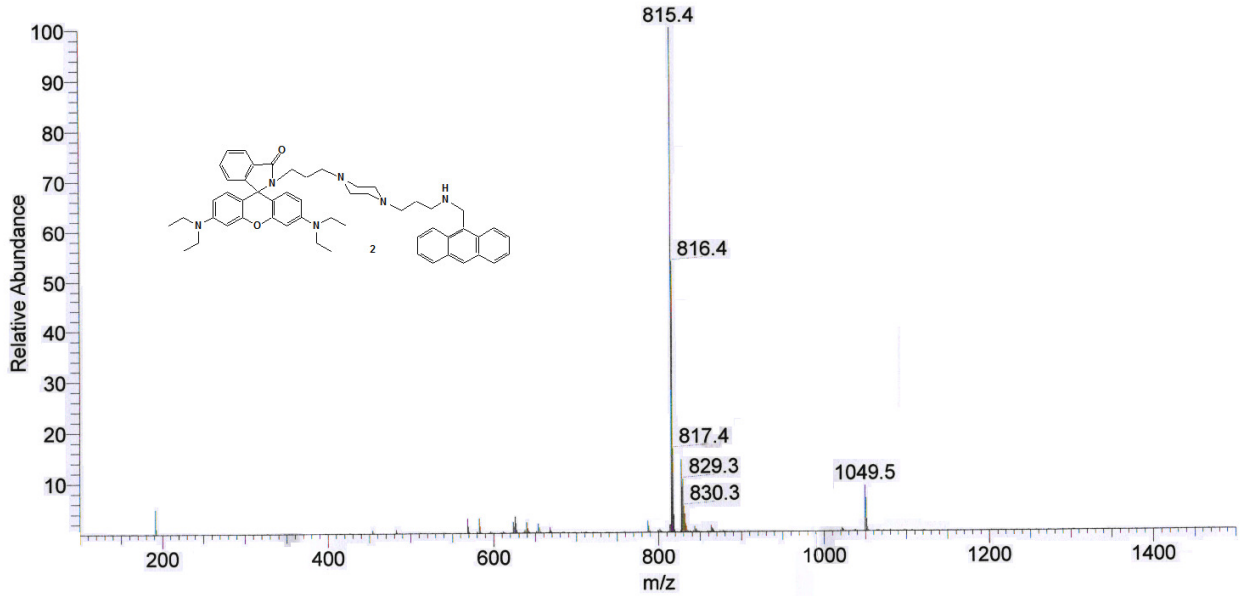

Fig. S21: ESI-MS of **2**.

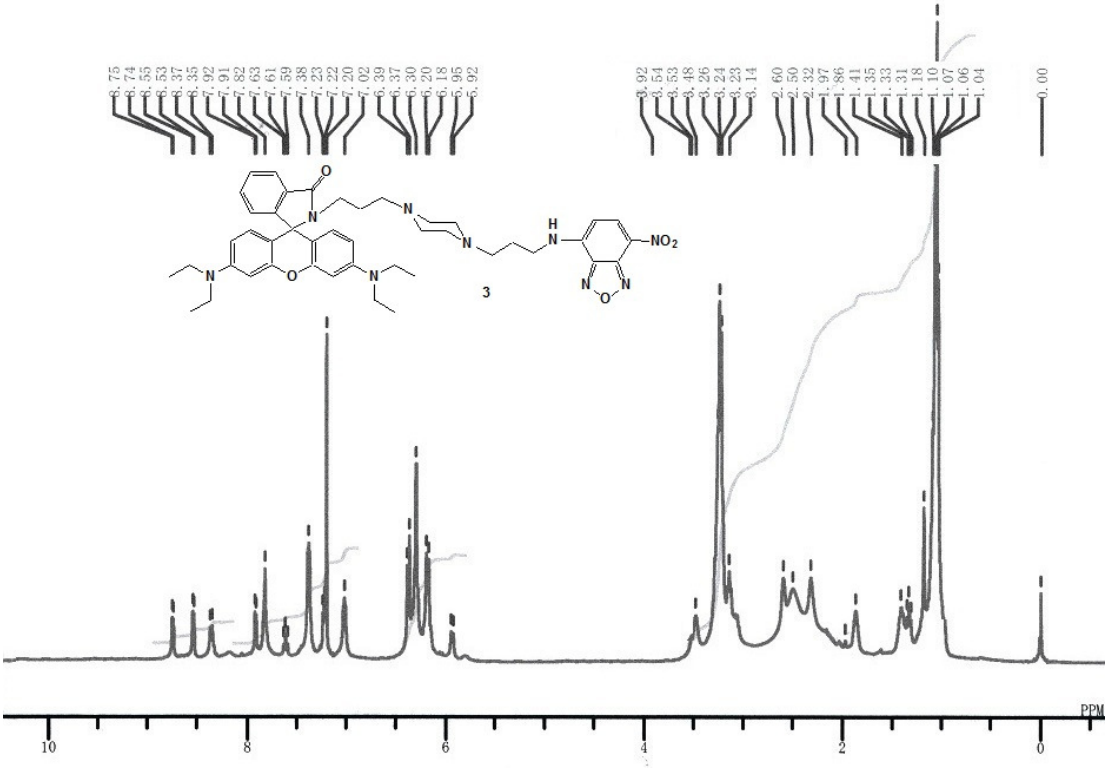

Fig. S22: ^{1}H-NMR spectra of **3** in $CDCl_3$

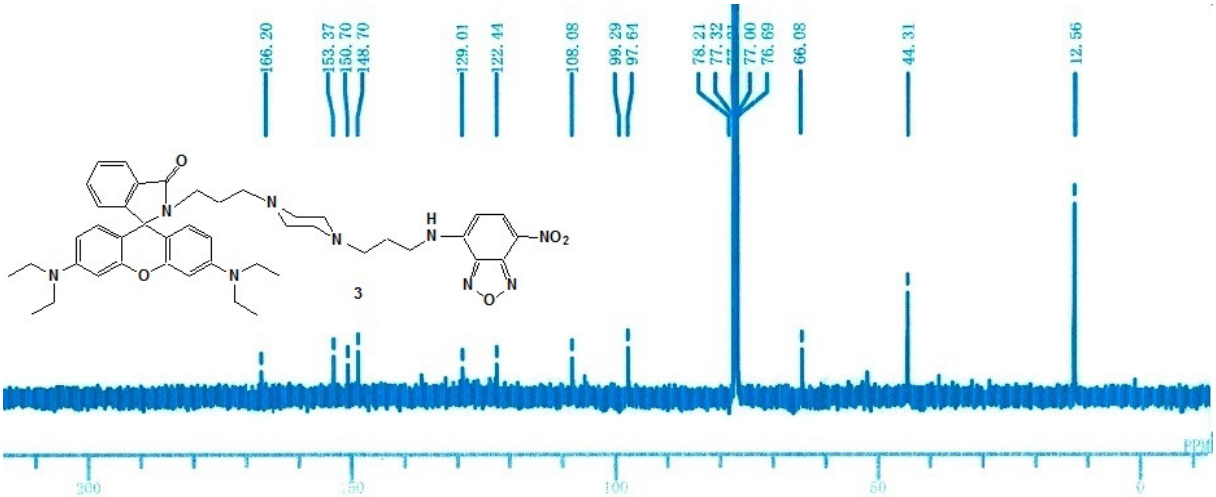

Fig. S23: ^{13}C-NMR spectra of **3** in $CDCl_3$

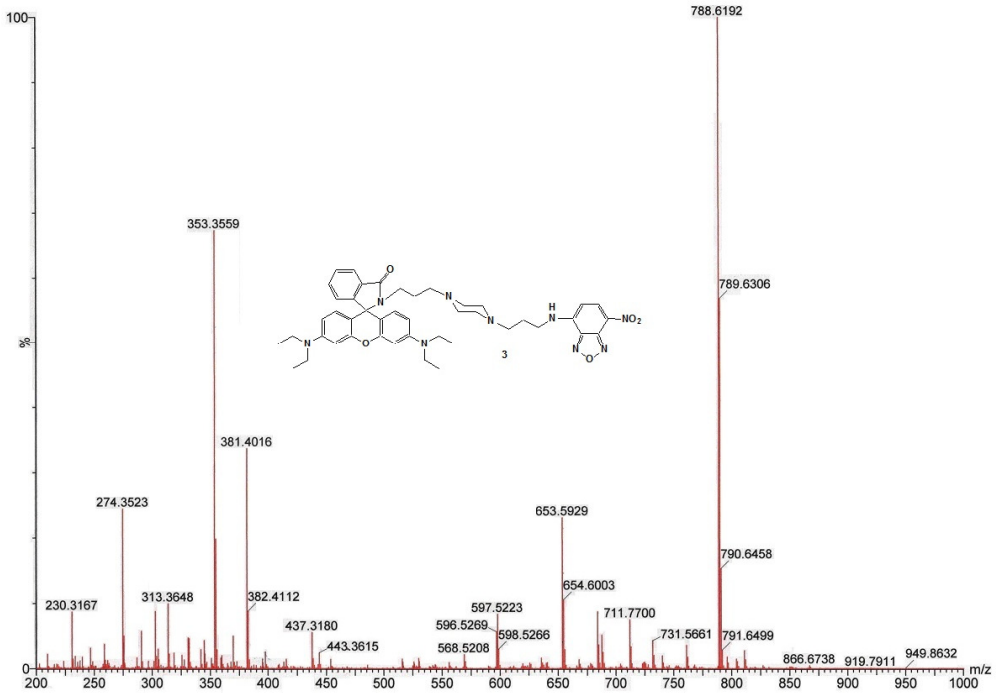

Fig. S24: ESI-MS of **3**.

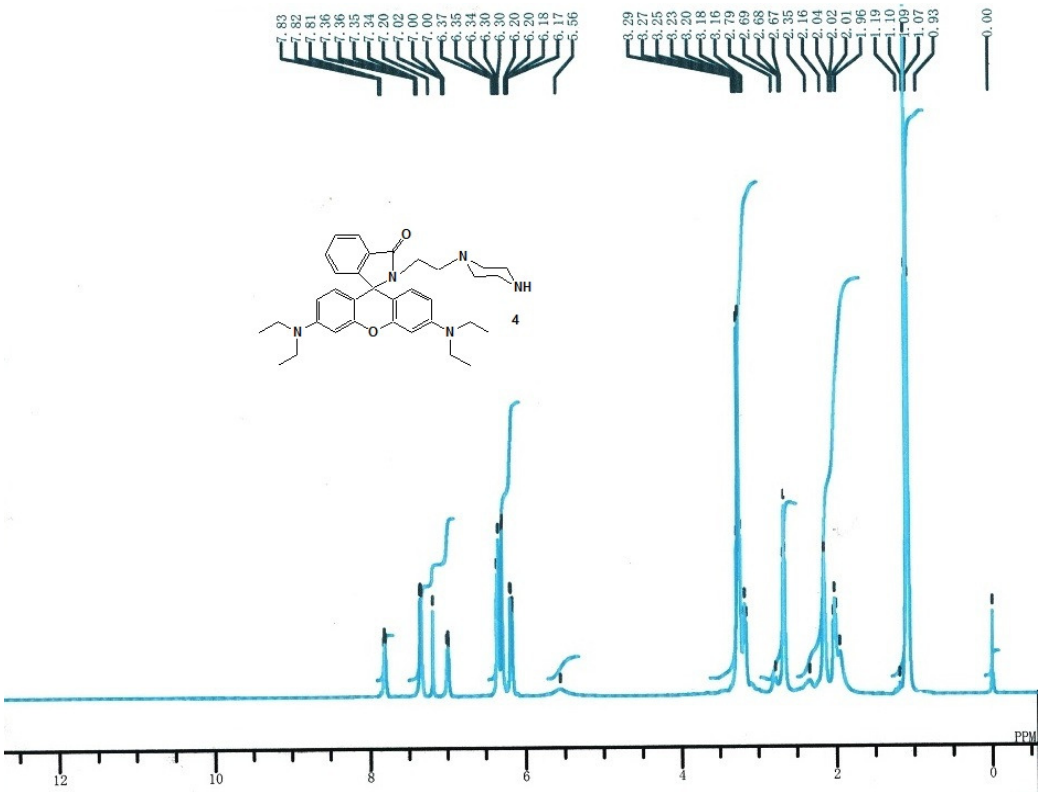

Fig. S25: ^{1}H-NMR spectra of **4** in $CDCl_3$

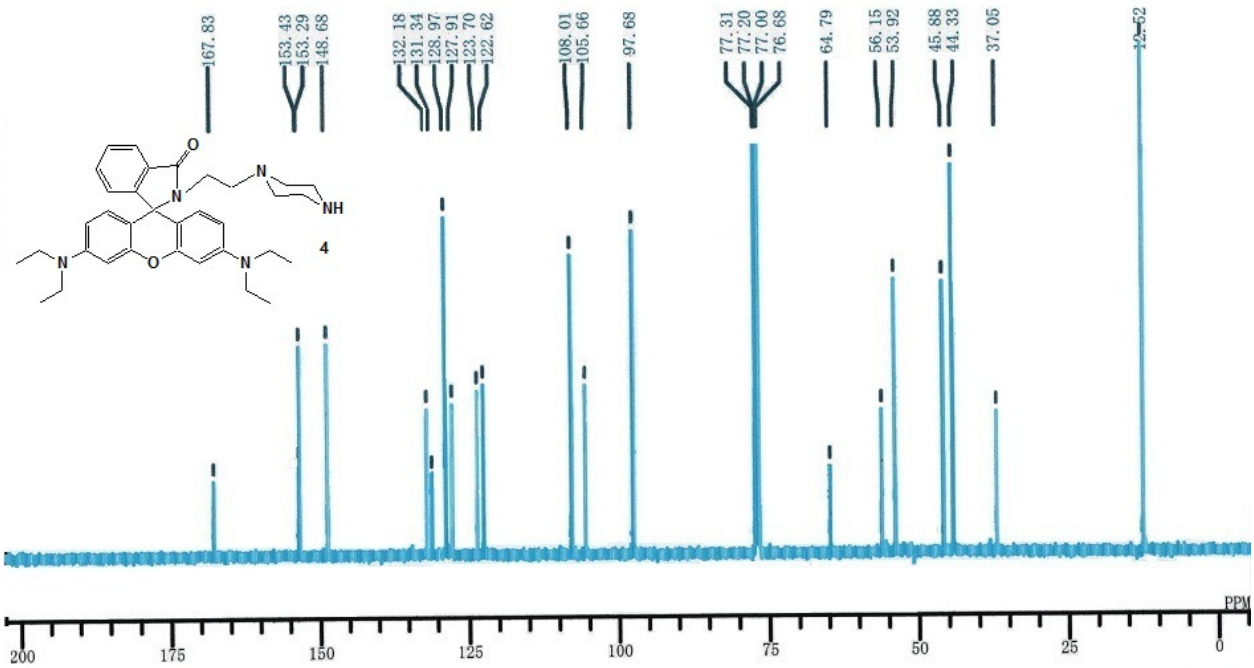

Fig. S26: ^{13}C-NMR spectra of **4** in $CDCl_3$

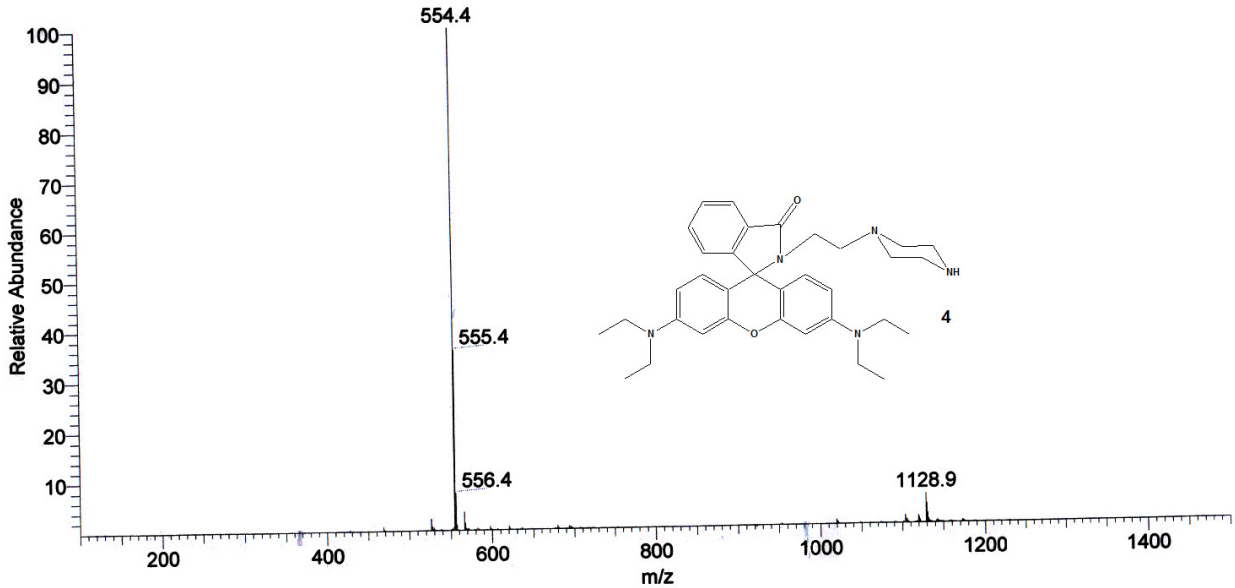

Fig. S27: ESI-MS of **4**.

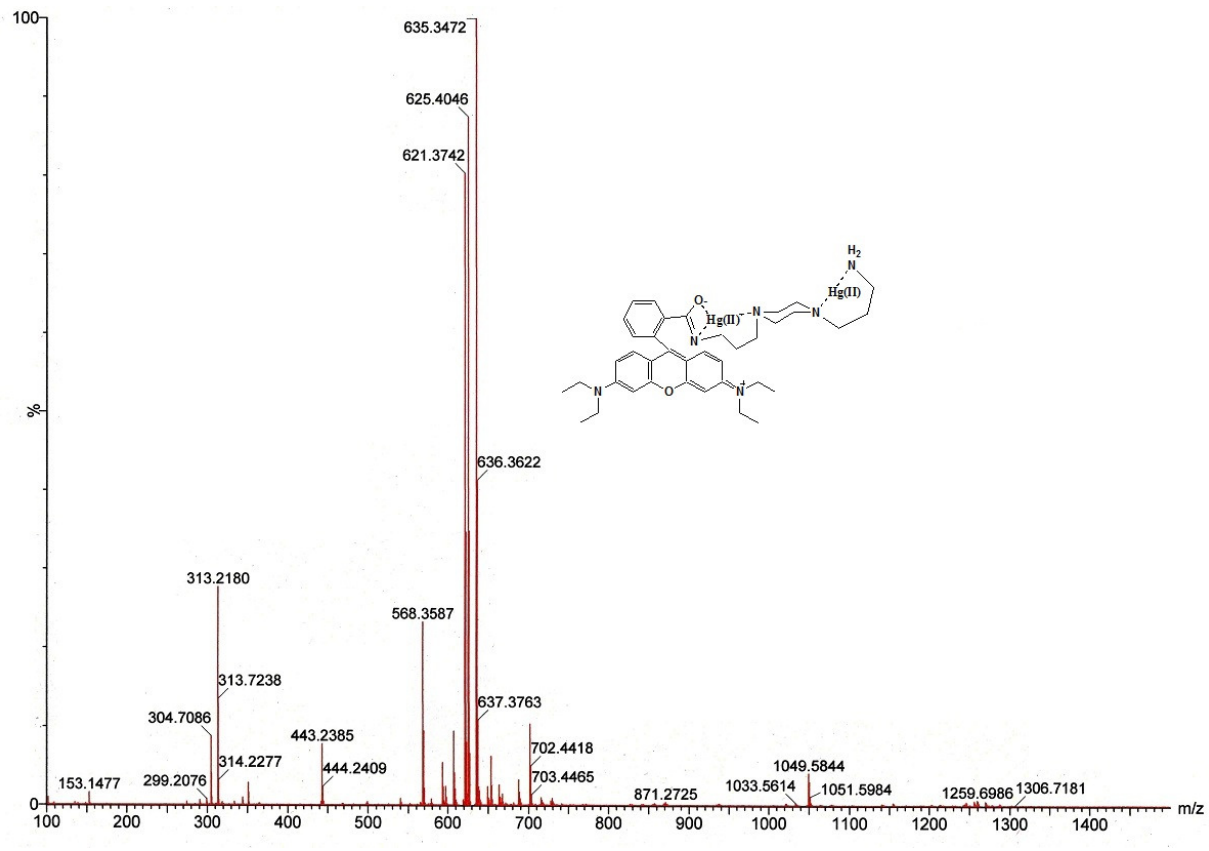

Fig. S28: ESI-MS of {**1⊂Hg(II)**}$_2$.